Electrolyte development for improved cycling performance of bismuth fluoride nanocomposite positive electrodes

Andrew J. Gmitter*, John Gural, Glenn G. Amatucci

Energy Storage Research Group, Department of Materials Science and Engineering, Rutgers, The State University of New Jersey, 671 US Hwy 1, North Brunswick, NJ 08902, USA

HIGHLIGHTS

► Bismuth fluoride nanocomposites examined in adiponitrile (ADN) electrolytes.
► Additive-free ADN superior to organic carbonate electrolytes.
► Additives explored to stabilize ADN on lithium but avoid interactions with BiF_3.

ARTICLE INFO

ABSTRACT

Interactions of the electrolyte with the bismuth fluoride nanocomposite positive electrode lead to capacity loss. When lithiated, the BiF_3 positive electrode is highly reactive with ethylene carbonate (EC) and other cyclic organic carbonates used for forming effective solid-electrolyte interphases (SEIs) on carbonaceous negative electrodes. This reactivity poses problems for the development of a Li-ion cell. The aim of this work was to formulate electrolytes that could enable the functionality of BiF_3 nanocomposite positive electrodes while also maintaining stability at the negative electrode/electrolyte interface. Adiponitrile (ADN) has been put forth as a compatible bulk solvent for the electrolyte, and a number of additives have been examined including cyclic organic carbonates, cyclic organic sulfur-containing compounds, and ethyl isocyanate. Along with an exceptional fundamental stability in the neat solvent, preliminary results demonstrated improved performance of BiF_3 nanocomposite positive electrodes in Li-ion compatible ADN-based electrolytes.

1. Introduction

The theoretical specific (302.3 Wh kg^{-1}) and high volumetric energy density (8042 Wh L^{-1}) coupled with a reasonably high potential ($\sim$3.2 V *vs.* Li/Li^+) make BiF_3 an attractive candidate for use as a rechargeable positive electrode material in Li-ion batteries [1,2]. When aggressively milled into a nanocomposite, this metal fluoride conversion material has demonstrated near-theoretical capacities and a relatively flat discharge plateau at moderate to very fast (3C) rates of cycling [2,3]. However, the BiF_3 nanocomposites have been plagued by rapid rates of capacity fade. Initially, the capacity loss was correlated with the decomposition of electrolyte solvents on the positive electrode. Nanodomains of Bi^0, formed as a result of the discharge (lithiation) of BiF_3, were

identified to catalyze the electrochemical reduction of cyclic organic carbonate solvents, notably ethylene carbonate (EC), from the electrolyte [2]. Recently, the species formed from the electrochemical reduction of EC at the positive electrode/electrolyte interface have been found to decompose during reconversion (delithiation). Subsequent formation of BiO_xF_{3-2x} through interactions of the Bi^0, LiF, and solid-electrolyte interphase (SEI) was evident [4].

Ethyl methyl carbonate (EMC) and dimethyl carbonate (DMC), examples of linear organic carbonate solvents, were not observed to decompose on the lithiated BiF_3 nanocomposites or on Bi films [2]. It was hypothesized that other straight-chained aprotic solvents such as dinitriles and 3-alkoxypropionitriles would behave similarly and offer pathways to significantly reduce or eliminate oxygen from the solvent. Novel electrolyte blends composed predominantly of EMC, adiponitrile (ADN, a dinitrile), and 3-methoxypropionitrile (3MPN) have recently been demonstrated in a 4 V Li-ion configuration [5]. When blended with suitable

soluble salts such as 1 M lithium bis(trifluoromethylsulfonyl) imide + 0.25 M lithium tetrafluoroborate (1 M LiTFSI + 0.25 M LiBF$_4$), none of these nitrile electrolytes were inherently able to stabilize the graphite negative electrode/electrolyte interface. This necessitated the addition of a small amount of the SEI-forming compounds, vinylene carbonate (VC) and monofluoroethylene carbonate (FEC) [5].

SEI additives are necessary to effectively passivate the negative electrode to prevent continual decomposition of the electrolyte. Additives are reduced on the negative electrode through reactions that typically involve the saturation of C=C double bonds and polymerization or the formation of radical anions through ring-opening mechanisms, both of which yield insoluble phases [6]. The SEI additive is typically reactive at potentials more positive than necessary for the electrochemical reduction of the main solvent(s) of the electrolyte; thus, the negative electrode is passivated before deleterious interactions of the electrolyte solvents can occur. Of the cyclic organic carbonates, VC was found to have the most positive reduction potential which is of great importance when considering it as an additive to promote SEI formation [7]. This would suggest that VC would be even more

susceptible than EC to electrochemical reduction on the catalytic Bi^0 formed during lithiation of BiF$_3$ nanocomposites. This suspected trait of VC led to the inclusion of cycling trials in which a variety of additives was compared. The additives were selected with regard to their molecular shapes, functional groups, solubility, and availability. The compounds are categorized by their functional groups, and key references are included with respect to their electrochemical properties and usage as additives in Li-ion cells (Tables 1 and 2).

The ideal SEI additive would stabilize a graphite, lithium, or alloy negative electrode and be electrochemically reduced at voltages below that of the operation of BiF$_3$. In essence, there would be no SEI formed *via* electrochemical reduction on the Bi metal that results from the lithiation of BiF$_3$. In this work, we first attempt to prove the intrinsic stability of BiF$_3$ in additive-free nitrile electrolytes by cycling *vs.* a counter electrode which is stable with the neat nitrile solvents (ADN and MPN). From there, we commence an investigation to identify an optimal class of additives that will stabilize the nitrile solvents *vs.* low voltage negative electrodes without resulting in deleterious effects on the BiF$_3$ nanocomposite conversion electrode material.
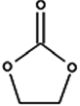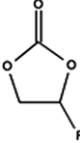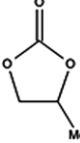
Table 1
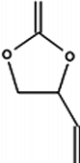Additives containing C=O functional groups.
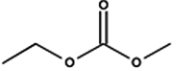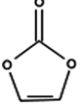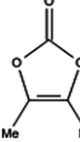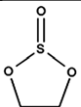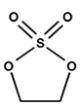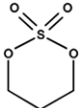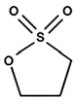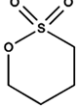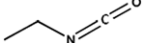
Common name	IUPAC name	Abbr.	CAS number	Chemical formula	Molecule [8]	Refs
Ethylene carbonate	1,3-Dioxolan-2-one	EC	96-49-1	C$_3$H$_4$O$_3$		[9]
Monofluoroethylene carbonate	4-Fluoro-1,3-dioxolan-2-one	FEC	114435-02-8	C$_3$H$_3$FO$_3$		[5,10]
Propylene carbonate	4-Methyl-1,3-dioxolan-2-one	PC	108-32-7	C$_4$H$_6$O$_3$		[9]
Vinyl ethylene carbonate	4-Ethenyl-1,3-dioxolan-2-one	VEC	4427-96-7	C$_5$H$_6$O$_3$		[11]
Ethyl methyl carbonate	Carbonic acid, ethyl methyl ester	EMC	623-53-0	C$_4$H$_8$O$_3$		–
Vinylene carbonate	1,3-Dioxol-2-one	VC	872-36-6	C$_3$H$_2$O$_3$		[9,12]
Dimethyl vinylene carbonate	4,5-Dimethyl-1,3-dioxol-2-one	DMDO	37830-90-3	C$_5$H$_6$O$_3$		[13]

Table 2
Additives containing S=O or N=C=O functional groups.

Common name	IUPAC name	Abbr.	CAS number	Chemical formula	Molecule [8]	Refs.
Ethylene sulfite	1,3,2-Dioxathiolane 2-oxide	ES	3741-38-6	$C_2H_4O_3S$		[14,15]
Ethylene sulfate or glycol sulfate	1,3,2-Dioxathiolane 2,2-dioxide	DTD	1072-53-3	$C_2H_4O_4S$		[16,17]
Propanediol cyclic sulfate	1,3,2-Dioxathiane 2,2-dioxide	PDCS	1073-05-8	$C_3H_6O_4S$		[18,19]
1,3-Propane sultone	1,2-Oxathiolane 2,2-dioxide	PS[a]	1120-71-4	$C_3H_6O_3S$		[20,21]
1,4-Butane sultone	1,2-Oxathiane 2,2-dioxide	BS	1633-83-6	$C_4H_8O_3S$		[22]
Ethyl Isocyanate	Isocyanatoethane	EtNCO	109-90-0	C_3H_5NO		[23,24]

[a] PS in this work is not propylene sulfite [4-methyl-1,3,2-dioxathiolane 2-oxide; 1469-73-4], an additive possessing the same chemical formula as 1,3-propane sultone. Propylene sulfite, also commonly abbreviated PS, was explored by Wrodnigg et al. [25].

2. Experimental

2.1. Materials synthesis

The methods of producing BiF_3 nanocomposite powders and Bi metal films have been described previously [2]. $LiCoO_2$ (LCO) tape electrodes were fabricated in a dry room (dew point $< -30\ °C$) by dispersing 0.600 g of LCO (C-22, Seimi), 0.320 g of polyvinylidene difluoride (PVdF) resin (Kynar Flex 2801, Arkema), 0.128 g of conductive carbon black (SuperP, Timcal), and roughly 0.4 g of dibutyl phthalate (DBP) in acetone. The suspensions were thoroughly mixed for 15–20 min before tapes were cast. After the acetone evaporated, the DBP plasticizer was extracted by soaking the tapes in diethyl ether. The tapes were vacuum dried overnight at 120 °C prior to transfer to a helium filled glovebox (<0.6 ppm H_2O, <0.1 ppm O_2, MBraun). The final active loading of LCO was 57.2 wt%.

With the exception of 1 M lithium hexafluorophosphate ($LiPF_6$) EC:DMC 1:1 v/v (Novolyte), all electrolytes were blended in-house in a helium filled glovebox. The salts and solvents utilized for blending base electrolytes were $LiPF_6$ (Ferro), LiTFSI (HQ-115, 3 M), $LiBF_4$ (Ferro), EC (Aldrich), DMC (Novolyte), EMC (Novolyte), 3MPN (Fluka), and ADN (Alfa). With the exceptions of 3MPN and ADN, these chemicals were battery or electrolyte grade, were delivered with <20 ppm H_2O, and were used as-received. The 3MPN and ADN initially had water contents of approximately 700 ppm and 820 ppm, respectively, as measured by coulometric Karl Fischer titration (Model 684, Metrohm). The 3MPN and ADN were treated in the following manner to reduce their water contents. Molecular sieves (3 Å, Aldrich) were vacuum dried overnight at 120 °C in glassware. The 3MPN and ADN were stored over the molecular sieves for 7 d with a ratio of 3 mL of solvent for each 1 g of molecular sieves. This treatment routinely yielded <10 ppm H_2O for the 3MPN and <15 ppm H_2O for the ADN.

Electrolytes were fabricated by adding either 1 M $LiPF_6$ or 1 M LiTFSI + 0.25 M $LiBF_4$ salts to the target solvents. The desired, typically 5–10 vol%, amount of additive VC (Ferro), EC, FEC (Novolyte), PC (Ferro), VEC (Aldrich), EMC, VC, DMDO (TCI America), ES (Aldrich), DTD (Aldrich), PDCS (Aldrich), PS (Aldrich), BS (Aldrich), and EtNCO (Aldrich) was then added to the electrolyte solution. For compounds that were solids at room temperature, the equivalent mass was added that would result in 10 vol% additive when dissolved into the ADN electrolyte.

2.2. Electrochemical characterization

2032-Type coin cells (Hohsen) were assembled with non-metalized (1 M LiTFSI + 0.25 M $LiBF_4$ electrolytes) or aluminized (1 M $LiPF_6$ electrolytes) stainless steel current collectors. For galvanostatic cycling trials, cells contained 5–6 mg of BiF_3 nanocomposite powder as the working electrode (WE), a porous membrane (Celgard) adjacent to the WE, and two layers of borosilicate glass fiber separator (GF/D, Whatman) saturated with electrolyte. The counter electrode (CE)/reference electrode (RE) for half cells was lithium foil (FMC). For Li-ion cells, the CE/RE was LCO tape with a $LiCoO_2:BiF_3$ weight ratio of 3.5:1.0. Galvanostatic trials of these cells were run on a BT2043 battery testing system controlled with MITS'97 software (Arbin). Trials were run at ± 15 mA g^{-1} BiF_3 between 2.00 and 4.50 V (CE/RE = Li) or -1.95 and 0.55 V (CE/RE = LCO) at 24 °C. The voltage plateau of LCO was 3.95 V vs. Li/Li$^+$.

Several three-electrode cells were assembled. These were used to justify the mass ratio and cycling parameters of the two-electrode BiF_3/LCO cells above. The WE was BiF_3, the RE was a ring (12.7 mm OD × 11.1 mm ID) of 316L stainless steel mounted to a partially bored-through stainless steel Swagelok body, and the CE was either LCO tape or Li. SS was used as a quasi-RE (qRE) after several failed attempts with Ag. When sitting in the cell at rest, the

open circuit potential of Ag vs. Li/Li$^+$ was nearly constant at 2.9 V, but during cycling of the BiF$_3$ nanocomposite, the Ag RE drifted from 2.9 V to 3.35 V vs. Li/Li$^+$. This swing was consistent with the plating of Bi^0 on the Ag RE. No such fluctuation was observed with the SS; thus, it was used as a qRE. The upper and lower potentials were established as 4.50 V and 2.00 V vs. Li or 0.55 V and −1.95 V vs. LCO. It is important to note that the RE was not used to control the applied current; the potential difference of the WE and CE was used for this purpose. Galvanostatic cycling trials were run at ±15 mA g^{-1} BiF$_3$ on a MacPile II (BioLogic) in a dry room.

Potentiodynamic scans in the 1 M LiTFSI + 0.25 M LiBF$_4$ ADN + 10 vol% additive electrolytes were run from the open circuit potential (approximately 3 V) to 1.00 V vs. Li/Li$^+$ at −1.25 mV/ 0.017 h on a MacPile II at 24 °C. Stainless steel coin cells were assembled in a similar manner as BiF$_3$ nanocomposite vs. Li half cells, but with a 12.7 mm disc of bismuth film serving as the WE.

3. Results and discussion

Galvanostatic cycling results of BiF$_3$ nanocomposite positive electrodes presented in Fig. 1 show that superior cycling was identified in LiPF$_6$ EMC vs. LiPF$_6$ EC:DMC. This result was consistent with previous observations, and highly reproducible [2]. The presence of EC (cyclic carbonate) as a 50 vol% co-solvent with DMC (linear carbonate), or VC (cyclic carbonate) as a 5 vol% cyclic carbonate additive to EMC (linear carbonate) had a detrimental impact on the long-term capacity retention of the BiF$_3$ nano-composite. The VC was included in this plot because EMC was observed as stable on Li but not on synthetic graphite negative electrodes in a Li-ion configuration; thus, a true Li-ion configura-tion employing BiF$_3$ positive electrodes would require an additive. The VC, though present to a far lesser extent, likely behaved in a similar manner as EC on the catalytically active Bi^0 formed during the lithiation of the BiF$_3$ [2]. In Fig. 1(b), the capacity values of EC:DMC and EMC faded more rapidly in the 1 M LiTFSI + 0.25 M LiBF$_4$ electrolytes than in the 1 M LiPF$_6$ electrolytes. The BiF$_3$ nanocomposites did not cycle well in EMC, ADN, and 3MPN-based electrolytes without a co-solvent or SEI additive present in the electrolyte. The 3MPN decomposed rapidly on the Li negative electrode (indicated by yellowish-brown discoloration of the elec-trolyte adjacent to the Li), and the ADN only endured several cycles before the cell was nonfunctional. The addition of 10 vol% VC aided in stabilizing the electrolytes from continual decomposition at the negative electrode. The ADN provided the best long-term capacity retention of the 1 M LiTFSI + 0.25 M LiBF$_4$ electrolytes containing 10 vol% VC, consistent with our previous studies reported on LiCoO$_2$ vs. graphite Li-ion cells [5].

From the LiPF$_6$ data (Fig. 1(a)), an electrolyte devoid of SEI additives was concluded to provide the best capacity retention. However, in the 1 M LiTFSI + 0.25 M LiBF$_4$ electrolytes (Fig. 1(b)), all of the electrolytes free of EC or VC were unstable on the Li negative electrode. It was not possible to determine how much of the capacity fade was inherent to the main solvent (i.e. EMC, ADN, or 3MPN) when VC was added. Therefore a methodology to examine the stability of the additive-free electrolytes vs. BiF$_3$ during cycling was needed.

In order to examine the electrolytes in a VC-free condition, LiCoO$_2$ (LCO) was used as the counter/reference electrode in a two-electrode Li-ion cell. LCO was greatly positive with respect to the reduction of the electrolyte solvents, and it was expected to be below the anodic limit of the solvents as well [9,26]. With LCO, no additive is required to enable stability of the electrolyte solvents as required with Li metal. In addition, the BiF$_3$ nanocomposites were in the fully charged condition and required Li$^+$ to be discharged (lithiated). The use of LCO enabled BiF$_3$ to be extensively tested in
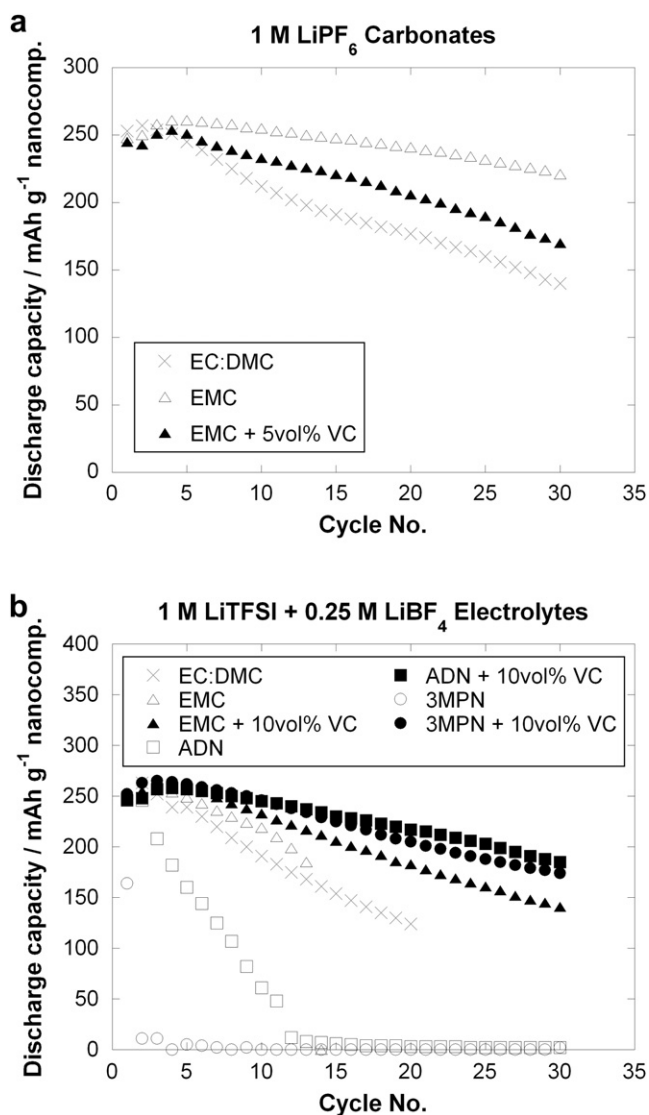
Fig. 1. Specific capacity of BiF$_3$ nanocomposites cycled galvanostatically between 4.50 V and 2.00 V vs. Li. (a) 1 M LiPF$_6$ carbonates. (b) 1 M LiTFSI + 0.25 M LiBF$_4$ electrolytes. Best cycling overall with 1 M LiPF$_6$ EMC and 1 M LiTFSI + 0.25 M LiBF$_4$ ADN + 10 vol% VC when using Li as negative electrode.

a Li-ion configuration. Any loss of Li$^+$ due to a parasitic reaction with BiF$_3$ will be accounted for and not replaced as is the case with Li metal half cells.

The data from three-electrode cells in which the CE was either Li foil (Fig. 2(a)) or LCO (Fig. 2(b)) and the qRE was SS are presented. After roughly 8 cycles, the three-electrode trials (Fig. 2) revealed that the potentials of the BiF$_3$ nanocomposite WE vs. SS qRE were similar for the two counter electrodes. The capacities were comparable, the potentials of BiF$_3$ vs. SS at the ends of lithiation and delithiation were almost identical, and the degrees of hysteresis in the reconversion of BiF$_3$ were comparable. The voltage profile (Fig. 2(a)) did indicate that the SS qRE drifted ∼100 mV during cycling trials. If the potentials of the Li CE and LCO CE vs. SS qRE (∼−3.11 V (Fig. 2(a)) and +0.82 V (Fig. 2(b))) are considered, despite running in two different cells, the combined average potential of LCO vs. Li was 3.93 V. This is completely consistent with the observed discharge potential of LCO in a typical half cell configuration. Overall, it was possible to cycle the BiF$_3$ in an unconventional fashion against LCO, and the three-electrode trials
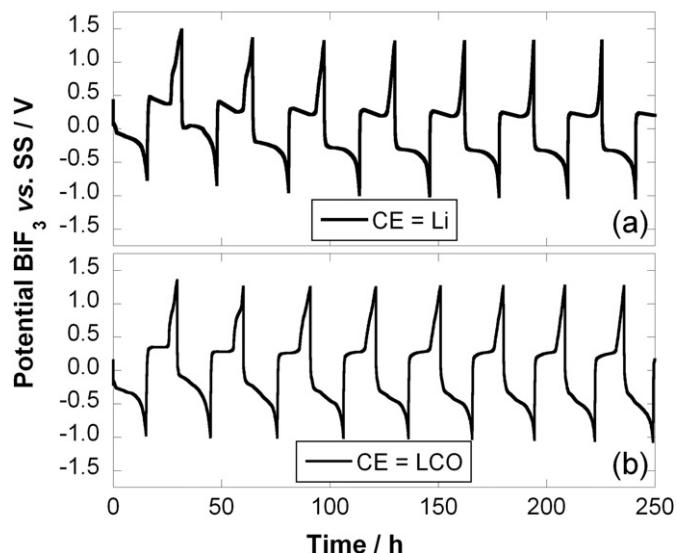
Fig. 2. Similarities observed in the voltage profiles of BiF_3 in three-electrode cells in which the counter electrode was Li (a) or LCO (b). WE: BiF_3 nanocomposite. RE: SS. Electrolyte: 1 M LiTFSI + 0.25 M $LiBF_4$ ADN. The electrolyte in (a) contained 10 vol% additive (VC) to stabilize the interface with the Li.

compatible electrolytes. Clearly, cycling in an electrolyte free of an additive (or co-solvent) susceptible to electrochemical reduction on Bi^0 provided superior results. It is, however, problematic for the development of a Li-ion cell of BiF_3 vs. a negative electrode such as synthetic graphite. The susceptibility of the additive to electrochemical reduction at potentials greater than the bulk electrolyte solvent(s) is the very property that is exploited when selecting functional additives. Without additives (or EC as a co-solvent), cycling of Li-ion batteries would not be possible, but with these types of additives, the interactions occurring with the BiF_3 nanocomposite lead to a significant degradation of performance.

Trials involving the VC-free electrolytes were momentarily cycled at a lower rate (± 3 mA g^{-1} BiF_3) around cycles 50–55 (Fig. 3). The ADN, and especially the 3MPN, electrolytes showed a fair amount of recovery of the discharge capacity suggesting a significant amount of the capacity loss is due to impedance increase rather than conversion material failure. Upon increasing the cycling rate to the original value (± 15 mA g^{-1} BiF_3), the ADN provided the best long-term capacity retention. The EMC, though previously identified to be quite non-reactive with the BiF_3, did not follow the same trend as the ADN and 3MPN electrolytes, but did offer improved performance relative to the EC:DMC. Importantly, the electrolytes containing VC exhibited poorer performance than their VC-free counterparts.

Of the electrolyte solvents considered in this study, the best long-term cycling performance of the BiF_3 nanocomposites was observed in ADN. While 1 M $LiPF_6$ EMC may have afforded slightly higher discharge capacities over the first 20 cycles, cycling in 1 M LiTFSI + 0.25 M $LiBF_4$ ADN (BiF_3 vs. LCO) has consistently been better to 100 cycles. Therefore, ADN was selected as the base electrolyte to which 10 vol% SEI promoting species was added. The SEI additives were required to stabilize the negative electrode/electrolyte interface to prevent the decomposition of the ADN on Li. The 10 vol% SEI additive concentration was established after blending 1 M LiTFSI + 0.25 M $LiBF_4$ ADN with 1 M LiTFSI + 0.25 M $LiBF_4$ VC in the following ADN:VC volumetric ratios and running galvanostatic cycling trials of BiF_3 nanocomposite half cells: 100:0, 95:5, 90:10, 75:25, 50:50, 25:75, and 0:100 v/v (Fig. 4). With the exceptions of the ADN:VC 100:0 and 0:100 electrolytes, the electrochemical cells were able to cycle in all the formulations containing both ADN and VC. An electrolyte composed solely of ADN
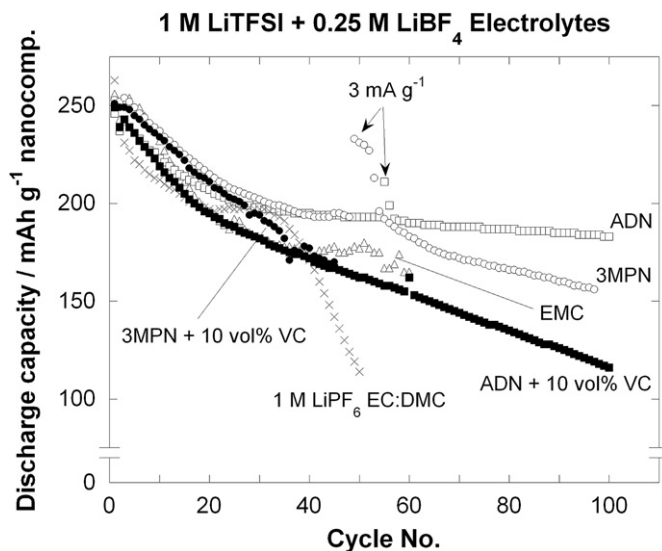
justified the series of two-electrode cells in which the WE was BiF_3 and the CE/RE was LCO.

The results of cycling BiF_3 nanocomposites in 1 M LiTFSI + 0.25 M $LiBF_4$ electrolytes against LCO CE/RE are presented in Fig. 3. Similarly to the 10 vol% VC data in Fig. 1(b), the ADN electrolyte exhibited the best long-term capacity. Remarkably, the discharge capacity of the BiF_3 nanocomposite in the additive-free ADN electrolyte was 183 mAh g^{-1} nanocomposite after 100 cycles with a flat cycling profile indicating cycling could continue for a considerable longer period of time. To date, this has been the best reported cycling of a BiF_3 nanocomposite positive electrode. It unequivocally demonstrated that good capacity retention was achievable with the BiF_3 nanocomposite utilizing a conversion mechanism to store energy, and it simultaneously highlighted the importance of identifying

Fig. 3. Specific capacity of BiF_3 nanocomposites cycled galvanostatically between 0.55 V and −1.95 V vs. LCO in various electrolyte solutions. Cycling was performed at 15 mA g^{-1} with intermittent 3 mA g^{-1} rates.
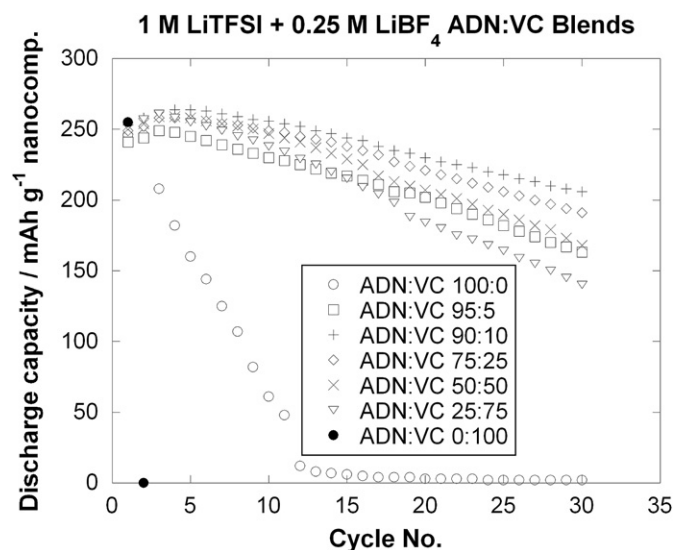

Fig. 4. Specific capacity of BiF_3 nanocomposites cycled galvanostatically between 4.50 V and 2.00 V vs. Li in 1 M LiTFSI + 0.25 M $LiBF_4$ ADN:VC electrolytes.

has already been established as unstable with respect to the Li negative electrode. The ADN:VC 0:100 reproducibly exhibited instability on the positive electrode at potentials exceeding 4.4 V vs. Li/Li$^+$ when paired with 1 M LiTFSI + 0.25 M LiBF$_4$. This observation was unexpected based on internal results with 1 M LiPF$_6$ VC in which cycling of BiF$_3$ to 4.5 V was achievable. In the case of LiPF$_6$, this could possibly be due to a protective decomposition of the LiPF$_6$ precluding the VC decomposition. While there is an abundance of SEI additive in the ADN:VC blends, if the interfaces are effectively passivated, additive decomposition should cease and the additive should remain in the electrolyte. 5 vol% VC in the ADN electrolyte seemed to be too low to effectively stabilize the negative electrode/electrolyte interface. Using 10 vol% concentration of various additives as a starting point in our investigations, the cycling performance of BiF$_3$ nanocomposite/Li metal half cells in ADN solvent were investigated in ADN + 10 vol% additive electrolytes (Figs. 5 and 6).

After 40 cycles, the two best ADN electrolytes contained the additives VC and FEC (Fig. 5). Both of these additives have been proven to form effective SEI on Li negative electrodes [12,15] as well as on synthetic graphite when added to nitrile solvents [2]. VC has already been shown to detrimentally impact the long-term cycling performance of BiF$_3$ nanocomposites in 1 M LiPF$_6$ EMC (Fig. 1(a)) and 1 M LiTFSI + 0.25 M LiBF$_4$ ADN electrolytes (Fig. 3) compared with EMC and ADN electrolytes free of additives. It was anticipated that in at least one of the other ADN electrolytes, the BiF$_3$ would perform better than in ADN + 10 vol% VC. Contrary to expectations, no improvement was observed with the other additives considered (Fig. 5). None of the sulfite, sulfate, or sultone compounds provided any benefit over the carbonate additives. However, it must be stressed that all conclusions are preliminary as we have not expanded the investigation to include variation in additive content (vol%) or voltage cutoff. Examination of the potential profiles of BiF$_3$ in electrolytes with the sulfur-containing compounds (Fig. 6) revealed decomposition of these additives at or above 2.0 V vs. Li/Li$^+$. This was especially apparent during the first discharge in ADN + 10 vol% ES, and evident in ADN + 10 vol% DTD, PDCS, PS, and

BS by the lack of sharpness of the potential profiles toward the end of second discharge (Fig. 6). The electrochemical reduction of these sulfur-containing compounds was also observed at or above 2.0 V vs. Li/Li$^+$ during potentiodynamic scans of Bi films (not shown). Thus, Bi^0 has been established as catalytic toward the reduction of cyclic organic compounds containing either C=O (and now) S=O functional groups. The S=O analogs of C=O cyclic organic compounds are likely more reactive with the Bi^0. In our work, the potential for ES reduction was observed to be more positive than EC. Theoretical investigations involving ES, DTD (reported as GS in [16]), EC, PC, and VC, have shown the reductive decomposition by lithium atoms in order of the most energetically favorable to be ES ~ DTD > EC ~ PC > VC for the first lithium addition [16]. This substantiated the reduction of cyclic organic compounds containing S=O functional groups at more positive potentials than those containing C=O functional groups.

Cyclic carbonates were expected to be poor candidates for electrolyte additives. EC, and to a lesser extent PC, have previously been established as reactive on Bi^0 and detrimental to the cycling performance of BiF$_3$ nanocomposites [2]. All the candidate additives were suboptimal, yet the best capacity retention was observed in ADN electrolytes containing cyclic carbonate additives based on the EC molecule (Table 1). Of the four molecules possessing a five-membered ring of 1,3-dioxolan-2-one, the VEC was most reactive on Bi^0, based on reaction potential. This has been attributed to the ethenyl (vinyl) group extending from the ring. VEC was found to decompose at approx. 2.4 V vs. Li/Li$^+$ during lithiation of the BiF$_3$ nanocomposite positive electrode (Fig. 6(e)). The extent of VEC decomposition was large enough to cause the specific capacity of the nanocomposite to exceed the theoretical maximum (266 mAh g^{-1}), and subsequent discharge capacities were drastically reduced. Of the additives EC, PC, and FEC, the galvanostatic cycling of BiF$_3$ nanocomposites was superior with 10 vol% FEC. It is unknown if the difference between the additives was attributable to their stabilities on the negative electrode or the different chemistries of the SEI formed on the BiF$_3$ nanocomposite. However, it is known that the decomposition of FEC results in a significant inorganic component of LiF at the negative electrode [5,10,27]. We have not examined whether decomposition to LiF is apparent at the higher voltages on Bi^0.

VC was observed to be the best SEI additive in the ADN electrolyte. If VC does form an SEI during the first lithiation of the BiF$_3$ nanocomposite, perhaps its ability to polymerize aids in forming an interfacial layer capable of accommodating the large volumetric expansion of the conversion electrode [28]. Also, perhaps a SEI that favors polymeric chains as opposed to carbonate moieties is more stable to anodic decomposition or has a much lesser tendency to interact with Bi^0 through a conversion mechanism as has been observed for SEI formed from EC [4]. DMDO, the most chemically similar molecule to VC in this study (Table 1), was completely unsatisfactory as an additive in the ADN electrolyte. It failed to remain stable to oxidative decomposition as evidenced by the prolonged voltage plateau above 4.3 V vs. Li/Li$^+$ (Fig. 6(h)).

The most intriguing additive was EtNCO (Fig. 6(n)) despite its inability to provide the best long-term cycling performance. It was among those samples which exhibited the most consistent voltage profiles and the least difference of the discharge and charge capacities. These attributes were common to EC (Fig. 6(b)), FEC (Fig. 6(c)), PC (Fig. 6(d)), EMC (Fig. 6(f)), VC (Fig. 6(g)), and EtNCO (Fig. 6(n)). These same additives yielded the best cycling of BiF$_3$ in ADN (Fig. 5). Compared with VC and FEC, the two best additives, EtNCO yielded a substantially lesser extent of charge capacity at potentials above 3.5 V during cycle 2 (Fig. 6(n)). Furthermore, the electrochemical reduction of EtNCO on a Bi film was identified to occur at approximately 1.7 V vs. Li/Li$^+$, a value more negative than
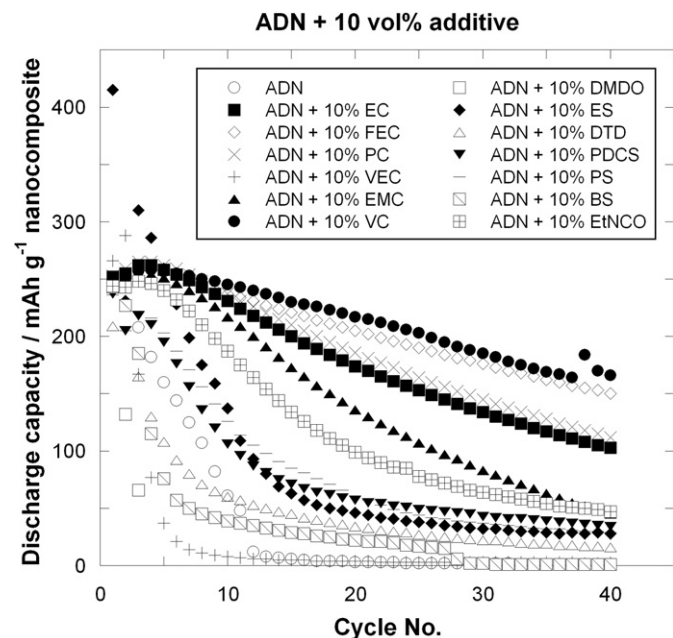

Fig. 5. Specific capacity of BiF$_3$ nanocomposites cycled galvanostatically between 4.50 V and 2.00 V vs. Li in 1 M LiTFSI + 0.25 M LiBF$_4$ ADN electrolytes.
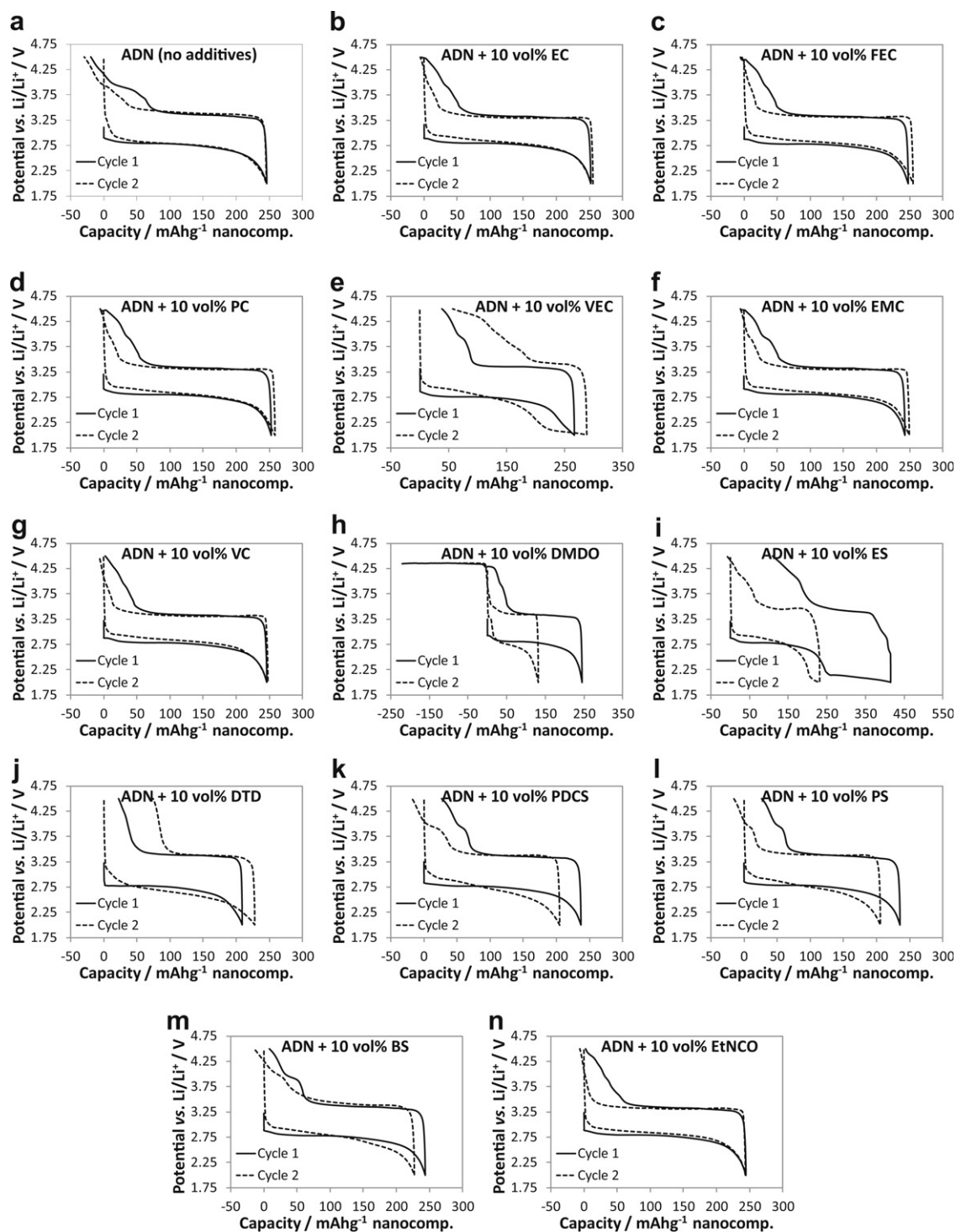
Fig. 6. Voltage profiles of BiF_3 nanocomposites plotted as a function of capacity. First two cycles shown for samples cycled galvanostatically between 4.50 V and 2.00 V vs. Li in 1 M LiTFSI + 0.25 M $LiBF_4$ ADN electrolytes. The theoretical capacity is 266 mAh g^{-1} nanocomposite. Note the different x-axis scale for panels (e), (h), and (i). (a) No additive, (b) 10 vol% EC, (c) 10 vol% FEC, (d) 10 vol% PC, (e) 10 vol% VEC, (f) 10 vol% EMC, (g) 10 vol% VC, (h) 10 vol% DMDO, (i) 10 vol% ES, (j) 10 vol% DTD, (k) 10 vol% PDCS, (l) 10 vol% PS, (m) 10 vol% BS, and (n) 10 vol% EtNCO.

the lower potential limit during galvanostatic cycling trials. During potentiodynamic scans (not shown), ADN + 10 vol% EtNCO exhibited the second lowest magnitude of current at 2.0 V of all the ADN electrolytes. The current was second only to the additive-free ADN electrolyte. Independent of whether EtNCO decomposes on the BiF_3 positive electrode, the poor long-term cycling performance

of BiF_3 nanocomposites in ADN + 10 vol% most likely arises from an ineffective stabilization of the lithium/electrolyte interface.

Overall, this study has not succeeded in improving the cycling performance of BiF_3 nanocomposite positive electrodes when paired with a negative electrode of low potential (i.e. Li) relative to that of the VC additives we have previously identified. However, it

has succeeded in expanding the list of solvents, whether as the main constituents of the electrolyte or as additives, to avoid when formulating electrolytes. The electrochemical reduction of cyclic organic solvents possessing C=O or S=O functional groups has been catalyzed on Bi^0, leading to rapid rates of capacity fade. Solvents containing ethenyl (vinyl) functional groups were also subject to decomposition on Bi^0. This has very serious repercussions and poses many difficulties to developing electrolytes suitable for use with bismuth nanocomposites. The vast majority of compounds identified for use as SEI additives in Li-ion cells are, in fact, based on these very same chemistries.

The additive must therefore be completely non-reactive with Bi^0 in its normally cycled voltage range or somehow withstand large volumetric changes, possible incorporation into the conversion material during delithiation, and/or possible anodic decomposition of the SEI during delithiation. Preliminary observations would suggest isocyanates to be prime candidates. On synthetic carbon, a widespread negative electrode in industrially manufactured cells, SEI layers were proven to form [23,24]. Regarding the BiF_3 nanocomposite positive electrode, preliminary results suggested the EtNCO to be relatively inert on Bi^0. EtNCO is a linear molecule with a different functional group than S=O, C=O, or C=C. Improved cycling of the BiF_3 nanocomposite, a fundamentally different type of positive electrode, requires the identification of electrolyte chemistries radically different than those presently established.

4. Conclusion

Cycling trials of BiF_3 nanocomposites in additive-free ADN showed that excellent capacity retention was attainable for a nanocomposite utilizing a conversion mechanism to store energy, and it simultaneously highlighted the importance of identifying compatible electrolytes. Superior results were yielded when the dinitrile electrolyte was devoid of any additives or co-solvents which are both susceptible to electrochemical reduction on Bi^0. The reactivity of additives with the BiF_3 nanocomposites poses problems for the development of a Li-ion cell. The ideal electrolyte additive for use in solvents such as ADN would (1) stabilize the negative electrode/electrolyte interface, (2) be non-reactive with the catalytic Bi^0, and (3) be able to withstand the relatively high positive potentials of the BiF_3 nanocomposite during reconversion.

Of the additives considered in this preliminary study, cyclic organic compounds containing C=O, S=O, or ethenyl (vinyl) functional groups were all subject to decomposition on Bi^0. Future trials with these compounds would involve lowering the additive concentration and studying the influence of the switching potential during discharge. From the observed voltage profiles (Fig. 6(n)) and its unique chemistry, EtNCO and other isocynates may be best suited as electrolytes additives compatible with BiF_3 nanocomposites.

References

[1] R.E. Doe, K.A. Persson, G. Hautier, G. Ceder, Electrochem. Solid-State Lett. 12 (2009) A125–A128.
[2] A.J. Gmitter, F. Badway, S. Rangan, R.A. Bartynski, A. Halajko, N. Pereira, G.G. Amatucci, J. Mater. Chem. 20 (2010) 4149–4161.
[3] M. Bervas, F. Badway, L.C. Klein, G.G. Amatucci, Electrochem. Solid-State Lett. 8 (2005) A179–A183.
[4] A.J. Gmitter, A. Halajko, P.J. Sideris, S.G. Greenbaum, G.G. Amatucci, Subsurface diffusion of oxide electrolyte decomposition products in metal fluoride nanocomposite electrodes, in preparation.
[5] A.J. Gmitter, I. Plitz, G.G. Amatucci, J. Electrochem. Soc. 159 (2012) A370–A379.
[6] S.S. Zhang, J. Power Sources 162 (2006) 1379–1394.
[7] E. Peled, D. Golodnitsky, in: P.B. Balbuena, Y. Wang (Eds.), Lithium-ion Batteries: Solid-Electrolyte Interphase, Imperial College Press, London, 2004, pp. 1–69.
[8] SciFinder (Web version), Chemical Abstracts Service/American Chemical Society, Columbus, OH, 2011 (Molecular structures drawn manually using CAS structure editor).
[9] K. Xu, Chem. Rev. 104 (2004) 4303–4417.
[10] I.A. Profatilova, S.-S. Kim, N.-S. Choi, Electrochim. Acta 54 (2009) 4445–4450.
[11] Y. Hu, W. Kong, H. Li, X. Huang, L. Chen, Electrochem. Commun. 6 (2004) 126–131.
[12] H. Ota, K. Shima, M. Ue, J. Yamaki, Electrochim. Acta 49 (2004) 565–572.
[13] M. Xu, L. Zhou, L. Xing, W. Li, B.L. Lucht, Electrochim. Acta 55 (2010) 6743–6748.
[14] G.H. Wrodnigg, J.O. Besenhard, M. Winter, J. Electrochem. Soc. 146 (1999) 470–472.
[15] R. Mogi, M. Inaba, S.-K. Jeong, Y. Iriyama, T. Abe, Z. Ogumi, J. Electrochem. Soc. 149 (2002) A1578–A1583.
[16] Y.-K. Han, S.U. Lee, J.-H. Ok, J.-J. Cho, H.-J. Kim, Chem. Phys. Lett. 360 (2002) 359–366.
[17] A. Sano, S. Maruyama, J. Power Sources 192 (2009) 714–718.
[18] A. Caiola, J.Y. Faudou, J.C. Sohm, Electrochim. Acta 17 (1972) 1401–1420.
[19] T. Nonaka, S. Kihara, T. Fuchigami, M. Bazier, Bull. Chem. Soc. Jpn. 57 (1984) 3160–3166.
[20] X. Zuo, M. Xu, W. Li, D. Su, J. Liu, Electrochem. Solid-State Lett. 9 (2006) A196.
[21] H. Lee, S. Choi, S. Choi, H.-J. Kim, Y. Choi, S. Yoon, J.-J. Cho, Electrochem. Commun. 9 (2007) 801–806.
[22] M.Q. Xu, W.S. Li, X.X. Zuo, J.S. Liu, X. Xu, J. Power Sources 174 (2007) 705–710.
[23] C. Korepp, W. Kern, E.A. Lanzer, P.R. Raimann, J.O. Besenhard, M.H. Yang, K.-C. Möller, D.-T. Shieh, M. Winter, J. Power Sources 174 (2007) 387–393.
[24] C. Korepp, W. Kern, E.A. Lanzer, P.R. Raimann, J.O. Besenhard, M. Yang, K.-C. Möller, D.-T. Shieh, M. Winter, J. Power Sources 174 (2007) 628–631.
[25] G.H. Wrodnigg, T.M. Wrodnigg, J.O. Besenhard, M. Winter, Electrochem. Commun. 1 (1999) 148–150.
[26] M. Ue, K. Ida, S. Mori, J. Electrochem. Soc. 141 (1994) 2989–2996.
[27] N.-S. Choi, K.H. Yew, K.Y. Lee, M. Sung, H. Kim, S.-S. Kim, J. Power Sources 161 (2006) 1254–1259.
[28] K. Tasaki, J. Phys. Chem. B 109 (2005) 2920–2933.